Tritium and Helium Production in Palladium Electrodes and the Fugacity of Deuterium Therein

John O'M. BOCKRIS
Chun-Ching CHIEN
Dalibor HODKO
Zoran MINEVSKI

ABSTRACT

An account is given of the massive production of tritium at a Pd electrode. Production continued for ~ 750 hours after which time it was arbitrarily curtailed. Production of T was found to cease every few days but could be resuscitated by increasing the overpotential of the electrode reaction. A logarithmic relation between the rate of tritium production and the overpotential of the electrode reaction was established. The Will-Cedzynska method of examining T contamination in specimens has shown that nothing above the background of T was detected if no D_2O had been electrolytically evolved on the Pd specimens concerned.

Helium production was found to accompany that of T. The He was analyzed by thermal expulsion and mass spectroscopy. No He^3 was found but He^4 was measured in nine specimens out of ten examined. Voids were also detected ~ 1 micron within the electrode. The excess tritium production on Pd co-deposited with deuterium was found.

Cracking and spreading of cracks is shown. An attempt was made to calculate the amount of hydrogen trapped in cracks and to calculate the standard free energy of trapping.

1. Introduction

For the studied phenomena it is desirable to make a set of simultaneous measurements of heat, neutrons, tritium, helium, x-rays and gamma rays. However, economic considerations have made it necessary to measure only one or two of these quantities.

The most obvious proof of cold fusion is the production of tritium from deuterium and we have gone principally in this direction. Recently, our group has observed an electrode which yielded T at ~ 10^4 times above the background. This paper deals with the production of tritium which continued for three weeks and was intentionally interrupted. Also, it was found that T production is accompanied with He production. Further, possible excess tritium production on Pd co-deposited with

FRONTIERS OF COLD FUSION

deuterium is considered as well as the speculations on the mechanism of reaction and conditions favorable to reach high fugacities inside the Pd electrode. Cracking of Pd electrode and trapping of hydrogen is also considered.

2. Methods

The principal method used in this investigation was a potentiostic one. The total potential applied to the cell was controlled and measured by a d.c. power supply. Cell potential, Pd electrode potential and current were measured by using Digital Multimeters and continuously monitored on XY-t recorders.

3.1. Production of tritium and helium

Experimental. The palladium electrodes were pre-treated by etching in dilute nitric acid and then treated electrochemically by applying a positive potential. The liquid scintillation counter was used for tritium measurements which was equipped with a chemiluminescence counter and indicated its own efficiency.

Helium analysis were done on palladium samples, which had shown tritium production. Also, analysis were done on platinum anode samples and non-electrolyzed Pd electrode samples. These were packed in solid CO_2 and sent to Rockwell International, Los Angeles, California for He^3 and He^4 analysis by mass spectrometry.

Results and Discussion. The usual procedure, for the initiation of tritium production was to charge the Pd electrode cathodically, at -0.05 V (vs. RHE) after the anodic pre-treatment. As shown in Fig. 1. there was no increase in tritium activity. The increase in cathodic direction triggers the reaction and a steady increase in tritium activity was observed. The initial, almost linear, relationship between tritium activity and time, is shown in Fig. 1, and this represents the results of two cells, A and B, run in parallel. The maintenance of a continuous increase in tritium activity, triggered by small increases in applied potential, has not been recorded previously though, T activity in a burst-like manner has been observed.

Tritium production reached its maximum of $3.8 \cdot 10^7$ T atoms s^{-1} cm^{-2} after 327 h of electrolysis, Fig. 2. The reaction was quenched at 406 h, when D_2O was added. Tritium production restarted again at 471 h of electrolysis with no potential increase.

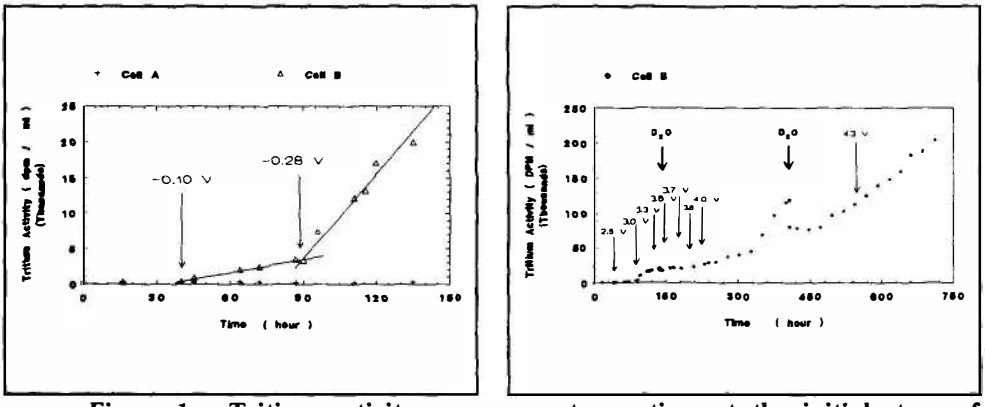

Figure 1. Tritium activity measurements vs. time at the initial stage of electrolysis: Cell with no (+) T in excess and ( ) high levels of T production.

Figure 2. Recording of the tritium events during one month of continuous tritium production in cell B. Arrows indicate voltage adjustments.

After the addition of heavy water tritium production ceased for two days. The reaction was quenched for the second time after 406 h of electrolysis and the decrease in T activity was observed due to dilution. An incubation period of 65 h was needed for the reaction to restart again.

From Figs. 1. and 2., four intervals of constant rate of tritium production may be recognized. A relation between overpotential and the rate of tritium production is shown in Fig. 3. The value of the slope is 4.5 ($F/(2 \cdot 2.303 \cdot RT) \sim 8.2$). In the sense of a Tafel slope, then, the present result $-\frac{4RT}{F}$.

Tritium contamination of Pd virgin material was also examined. A summary of results is shown in Table 1. For this purpose virgin Pd was dissolved in aqua regia and liquid scintillation analysis of distilled samples were done. The method used, was the one developed by F. Will and K. Cedzynska and both, the closed apparatus for dissolution of Pd as well as the one for distillation were similar to those described in ref. [1].

Table 1. Tritium analysis of the bulk of virgin Pd rod.

Sample # 01	Sample # 02	Sample # 03
$4 \pm 3 \cdot 10^8$ T-atoms/g Pd	$3 \pm 3 \cdot 10^8$ T-atoms/g Pd	$4 \pm 3 \cdot 10^8$ T-atoms/g Pd

It is important to note that tritium measurements before the start of electrolysis were also done and the results are shown in Table 2. No increase in T activity was observed in the electrolyte after anodic pre-treatment.

Table 2. Typical tritium activity analysis of the 0.1 M LiOD electrolyte before and after anodic pretreatment.

T-activity before anodic pretreatment DPM / ml	T-activity after anodic pretreatment DPM / ml
12 ± 3	12 ± 3

An attempt was made to restart T production after ceasing the electrolysis. All tritium results are summarized in Table 3. However, no further T production was found.

After intentionally stopping the electrolysis, a Pd electrode, which produced tritium, was transferred into liquid nitrogen and was kept there for one week. Then it was removed and cut into 5 pieces for further analysis. Fig. 4. shows how the Pd electrode was cut and the position of cut discs used for He^3 and He^4 analysis as well as for some other analysis.

Disc #5 was cut for He^3 and He^4 analysis.

All samples, with and without thermal treatment showed positive findings of He^4. The data in Fig. 5. represent the amounts of He^4 released by the specimens that exceeded the average amount released or desorbed during the analysis of the Rockwell control specimens. Excess of He^4 was observed in 9 out of the 10 electrolyzed palladium samples from electrode which produced tritium. In the case of He^4 there was no interference as far as the production of an HD artifact is concerned. However, an HD artifact interfered with the signal for He^3. It is assumed that the interference with He^4 does not occur because of better resolution between He^4 and hydrogen isotope signals.

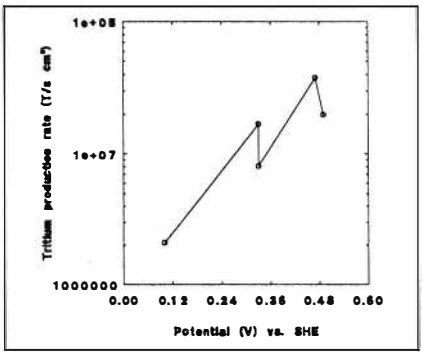

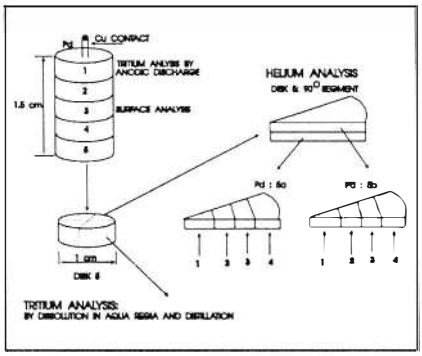

Figure 3. Tritium production rate dependence on electrode overpotential.

Figure 4. Pd electrode which produced tritium: cutting diagram and annotation of samples used in subsequent analysis.

Table 3. Summary of tritium results.

T_{total} in ELECTROLYTE	T in GAS PHASE (assuming $T_g/T_l=5$)	T in Pd (by dissolution in aqua regia)	T in Pd (by anodic discharge method)
$1.6 \cdot 10^{14}$ T-atoms or $1.5 \cdot 10^{13}$ T-atoms/g or $2.5 \cdot 10^{13}$ T-atoms/cm^2	$8.1 \cdot 10^{14}$ T-atoms or $5.4 \cdot 10^{13}$ T-atoms/g or $1.2 \cdot 10^{14}$ T-atoms/cm^2	$5.1 \cdot 10^{9}$ T-atoms/g Pd (or total in Pd=$7.6 \cdot 10^{10}$ T)	$8 \cdot 10^{9}$ T-atoms/g Pd (or total in Pd=$1.2 \cdot 10^{11}$ T)
TOTAL AMOUNT OF T PRODUCED (ELECTROLYTE, GAS, BULK)		$\sim 10^{15}$ T-atoms or $6.9 \cdot 10^{13}$ T-atoms/g or $1.5 \cdot 10^{14}$ T-atoms/cm^2	

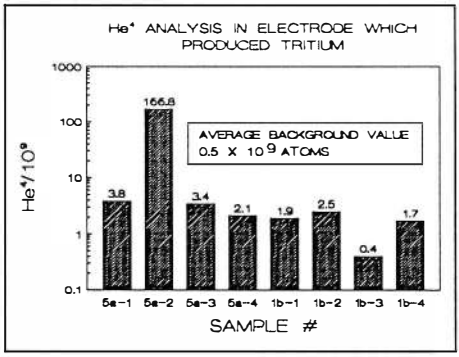

Figure 5. He^4 analysis in electrode which produced tritium.

Thus, were needed samples were thermally pre-treated prior to analysis. In this way mass spectra collected were free from any interference of residual hydrogen isotopes.

3.2. Tritium produced on Pd co-deposited with deuterium

Experimental. Another type of experiment was performed in order to check the possible excess of tritium production. The electrolysis started at low current densities of 2.5 mA cm^{-2} in order to avoid a too fast Pd dendrite growth. Within the next 5 hours the current density was increased to 25 mA cm^{-2}, which was followed by a large potential change from c. -0.02 V to -0.8 V vs. RHE.

Results and discussion. If the obtained results are compared with previously published data for deuterium evolution on Pd [2] it is then obvious that Pd deposition took place with simultaneous deuterium evolution at high overpotentials. Also within the first 40-50 hours of electrolysis a highly dendritic layer of Pd was visible at the electrode and was approximately 2-3 mm thick.

It is known that a change in tritium concentration occurs due to the additions of fresh D_2O containing background levels of T and due to the removal of tritium by electrolysis. The later depends on the isotopic separation factor of tritium and deuterium, S, [3]:

$$\frac{n_T(t)}{n_T(0)} = S - (S - 1)\exp(-\frac{t}{\tau}) \qquad (1)$$

This equation assumes that the amount of tritium added to the solution is equal to the rate of tritium removal by electrolysis. In equation (2) .. is the tritium build-up time constant given with the following expression:

$$\tau = \frac{S n \cdot V}{R} \qquad (2)$$

where n is the concentration of D_2O in mole dm^{-3}, V is the volume of the cell in dm^3 and R is the rate of deuterium production in the solution, R = I/2F. The D/T separation factor on Pd is in the range of 1.7 to 2.2, and in this case a value of 2 was taken.

Fig. 6., shows the change in tritium concentration, both for the liquid and gas phases during the two weeks of electrolysis. For comparison, theoretical lines as calculated from equations (1) and (2) are also shown in this figure. A burst type of excess tritium production was observed in the gas phase. At the same time or with the delay a burst in the solution phase occurred. A summary of T production observed in four out of six investigated cells is given in Table 4. The only cell which did not demonstrate excess tritium production is cell E shown in Fig. 7.

It is important to note that in both cells where no excess of T was found, a Cambridge D_2O was used. However, in previous cold fusion-positive results an Isotech D_2O was used [4] as in the cells A, B and C.

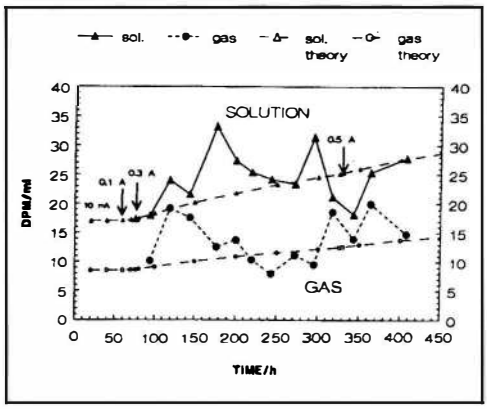

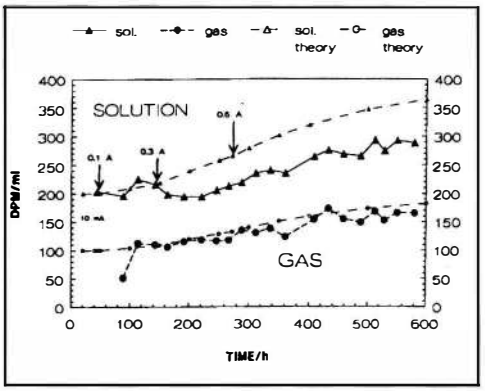

Figure 6. CELL A: T bursts in the liquid and gas phases during 2 weeks of electrolysis in 0.05 M $PdCl_2$/0.3 M LiCl; dashed lines-theoretical values.

Figure 7. CELL E: T bursts not observed during the two weeks of electrolysis.

Table 4. Summary of excess tritium findings in cells A, B, C and D.

CELL	INITIATION TIME hours	BURST #	BURST DURATION hours	GAS PHASE T_g/T_{gth}	SOLUTION T_s/T_{sth}	RATIO T_g/T_s	COMMENT
A	35	1	120	2.1	1.6	0.83	bursts in gas phase precede bursts in solution
		2	80	1.8	1.3	0.93	
B	32	1	140	2.4	2.1	0.67	both gas and liquid above T_{th} during whole experiment
		2	70	1.6	1.7	0.51	
C	17	1	130	2.1	1.7	0.80	gas phase constantly ca 80% above T_{th}
		2	90	1.6	1.2	0.91	
D	25	1	135	1.5	1.0	1.52	T bursts both in gas and liquid phases; decreased with time of electrolysis

3.3. Presence of D in voids

Experimental. The potentiostatic current proportional to the rate of deuterium permeation is measured in a specially constructed permeation cell. Here, deuterium is evolved on the cathodic side of a bi-electrode, Pd membrane, and the permeating deuterium is oxidized, anodically on the other side.

Results and discussion. Working on the permeation of deuterium through the Pd metal as a function of time, results, have been observed, which indicate the embrittlement and damage of Pd. Time variation of the current is interpreted in terms of changes in the metal structure caused by absorption of deuterium. This method allows the determination of permeation current, P, diffusion coefficient, D, and the solubility of hydrogen corresponding to a certain fugacity which in turn corresponds to the overpotential according to following equations:

$$D = \frac{0.693 \cdot L^2}{t_{\frac{1}{2}}} \qquad (3)$$

$$P_\infty = \frac{FD(C_0 - C_L)}{L} = \frac{FDC_0}{L} \qquad (4)$$

Fig. 8. shows spreading of cracks. The first and the second micrograph are taken after 2 and 4 hours of electrolysis on the mirror polished Pd disc, from the outer area of the electrode inward. The rate of crack spreading corresponds to the diffusion coefficient of deuterium into the Pd metal. The third one shows the appearance of cracks after etching in nitric acid.

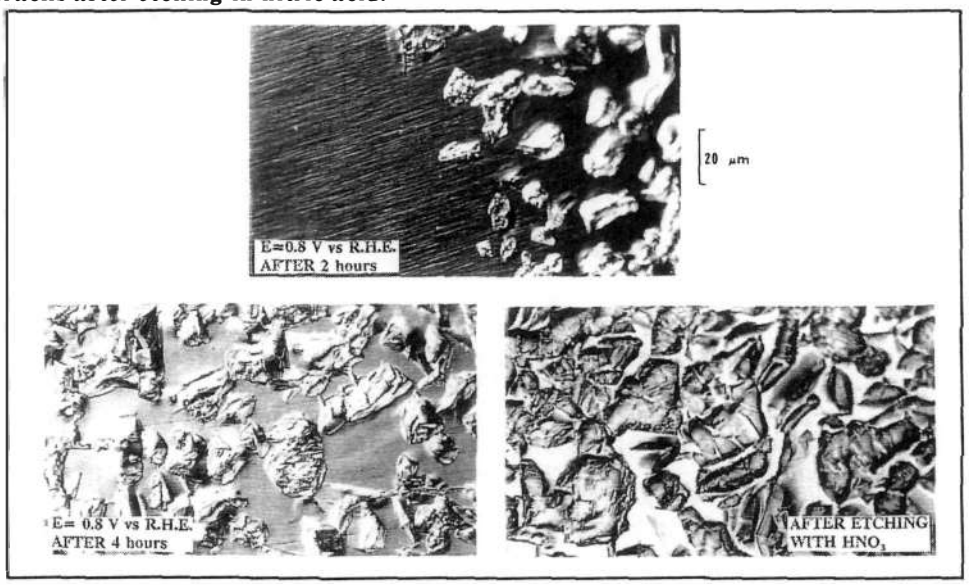

Figure 8. Micrographs, obtained by differential interference contrast microscopy, of mirror polished Pd after 2 and 4 hours of hydrogen evolution, and after etching in HNO_3.

In Fig. 9. the permeation of deuterium as a function of applied potential in the solution of pH=13. Each point represents the steady state current obtained at the corresponding potential. The increase in permeation current is observed with the subsequent increase in potential. A decrease in permeation current is seen from Fig. 8. and this clearly indicates that at higher overpotentials the permeation of deuterium is associated with the onset of deuterium embrittlement.

The permeation-time transients below and at critical potential are shown in Fig. 10. At lower potentials a typical permeation-time transients are obtained, without any noticeable difference except in the permeation value. These transients are reproducible. However, it was found that there is a threshold value of the deuterium potential when the permeation-time transient exhibits a maximum, Fig. 10., and when an attempt to repeat a transient has failed.

The question what happens at this so-called critical potential has already been addressed [5] and it is assumed that at this potential a critical concentration of D is dissolved and as this level is reached, some kind of change in metal lattice occurs. Taking in account the fugacity of D_2 in the metal, it seems reasonable to conclude that the process corresponding to the maximum of the permeation-time relationship is the spreading of microcracks.

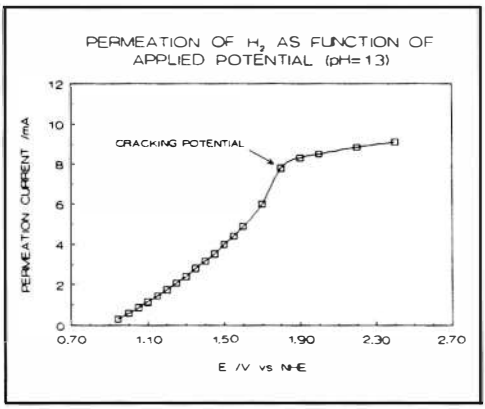

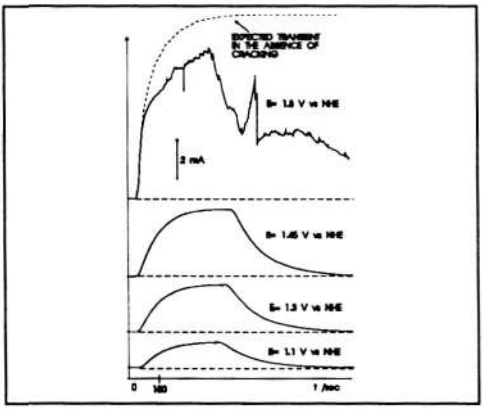

Figure 9. Permeation of H_2 as a function of applied potential.
Figure 10. Permeation-time transients exhibiting normal behavior and cracking.

By following the model of Bockris and Subramanyan [6] of this anomalous permeation it is possible to determine the quantity of trapped hydrogen and the standard free energy of trapping. The trapping reaction can be represented as

$$D + \square \rightarrow D_{tr} \tag{5}$$

and the equilibrium is attained when

$$C_{D,tr} = K^1 C_{\square} C_{D,L} \tag{6}$$

where $C_{D,tr}$ and $C_{D,L}$ is the concentration of D in traps and in the lattice sites, respectively. $C_{\square}$ is the concentration of unfilled traps, while K^1 is the equilibrium constant. For a given concentration of lattice D, the number of filled traps at equilibrium will be proportional to $C_{D,L}$ and so

$$C_{D,tr} = KC_{D,L} \qquad K = K^1 C_{\square} \tag{7}$$

The differential equation which describes the lattice diffusion with trapping is based on the fact that diffusion from one trapping site to another does not occur by direct jump without the intermediate stage of diffusion through the lattice sites:

$$\frac{\partial C_{D,L}}{\partial t} + \frac{\partial C_{D,tr}}{\partial t} = D\frac{\partial^2 C_{D,L}}{\partial X^2} \tag{8}$$

and by taking in account previous equations for $C_{D,L}$ and $C_{D,tr}$ it follows that

$$\frac{\partial C_{D,L}}{\partial t} + \tau K\frac{\partial C_{D,L}}{\partial t} = D\frac{\partial^2 C_{D,L}}{\partial X^2} \tag{9}$$

and

$$\frac{\partial C}{\partial t} = \frac{D}{(1 + \tau K)}\frac{\partial^2 C}{\partial X^2} \tag{10}$$

The last equation can be solved assuming that the entry of D into the lattice is a fast process and that the trapped D will always be in equilibrium with lattice dissolved hydrogen (C_0) and hence the numerical constant τ is 1. The boundary conditions are:

$$at\ X=0,\ for\ t>0,\ C = (1 + K)C_0 \tag{11}$$

and

$$at \quad X=L, \quad for \ t>0, \quad C=0 \tag{12}$$

The solution is

$$C(X,t) = (1 + K)C_0 \ (A - B) \tag{13}$$

where

$$A = \sum_{n=0}^{\infty} (-1)^n \ erfc \ \frac{(X + 2nL\sqrt{1 + \tau K})}{2\sqrt{Dt}} \tag{14}$$

and

$$B = \sum_{n=0}^{\infty} (-1)^n \ erfc \ \frac{(-X + 2L + 2nL)\sqrt{1 + \tau K}}{2\sqrt{Dt}} \tag{15}$$

and the permeability is given as:

$$P_{tr} = \frac{DfC_0}{L} \frac{2}{\pi^{\frac{1}{2}}} \left(\frac{L^2}{Dt}\right)^{\frac{1}{2}} \exp\left(-\frac{L^2(1 + \tau K)}{4Dt}\right) \tag{16}$$

The last equation shows that at relatively short times the trapping permeation is smaller than normal permeation. Also, once the trapping is switched on the permeability decreases from the normal one and gives rise to the prominent hump in the build-up permeation transients, Fig. 10. From this figure it can also been seen what would be an expected normal transient if cracking did not occur (dashed line). The steady state permeability was obtained after 90 minutes.

In order to obtain the total amount of trapped deuterium the area between the extrapolated and the actual transient is calculated for charge. The trapping constant, K, is calculated by knowing the charge of trapped hydrogen, Q, the permeation area, A, thickness of the membrane, L, C_0 and C_{crit} which is the solubility of H calculated from the transient which does not and which exhibits the cracking, respectively. Thus, from

$$K = \frac{2\,Q}{AL(C_0 - C_{crit})} \tag{17}$$

and

$$C = \frac{PL}{zFD} \tag{18}$$

where P is permeation and D diffusion coefficient, $D=1 \cdot 10^{-6}$ cm^2 sec^{-1}.
It turns out that $C_0=2.38 \cdot 10^{-3}$ mole cm^{-3}, $C_{crit} \approx 1.97 \cdot 10^{-3}$ mole cm^{-3}, Q = 45 C, A = 1 cm^2, L= 0.025 cm. And so the trapping constant is K=0.93.

Now, in order to get the equilibrium constant the concentration of traps is calculated assuming that the density of microcrack or Stroh cracks is 10^8/cm^2 [6]. Further from Fig. 8. the length and the width of the cracks is taken to be approximately 10^{-3} and 10^{-4} cm, respectively. Thus, the internal surface are of the crack and the number of metal atoms therein is calculated. Lastly, the density of traps per cm^3 and concentration of traps is calculated. So, the C of traps is $3 \cdot 10^{-6}$ mole dm^{-1}. Hence, the equilibrium constant is calculated to be $K^1=3.1 \cdot 10^5$. From here then the standard free energy of trapping is obtained as

$$\Delta G = -RT \ln K^1 = -31.33\ kJ\ mole^{-1} \quad (19)$$

which is equivalent to - 7.5 kcal $mole^{-1}$. This value seems to be in good agreement with the standard free energy of solubility of hydrogen in Pd found by Fullenwider to be - 4 kcal $mole^{-1}$, [7].

From C_{crit} and Sievert's low it is possible to calculate the critical pressure needed to expand a microcrack:

$$p_{D_{2crit}}^{\frac{1}{2}} = \frac{C_{crit}}{K_s} \quad (20)$$

where K_s is Sievert's constant equal to $8.8 \cdot 10^{-9}$ $mole^{-1/2}$. Thus, for the above value of C_{crit} the value obtained for p_{crit} is $5 \cdot 10^4$ atm.

4. Discussion

It is not unusual to observe high Tafel slopes [2]. The logarithmic dependence of the rate upon overpotential and the rational slope indicates that the rate determining step for the passage of tritium into solution is a charge transfer mechanism which probably involves a reverse proton discharge mechanism. An explanation for the high tritium production on Pd, based on the influence of the amount and the type of impurities on the mechanism of deuterium evolution reaction on Pd surface has already been proposed [2,4,8].

It is important to note that according to the above calculations, deuterium is mostly located in voids and cracks and not in the bulk of the electrode. From the experimental results and Sievert's law it is shown that the critical pressure to expand the microcrack is $5 \cdot 10^4$. This is in good agreement with the critical pressure of $3 \cdot 10^4$ [8] used to calculate the fugacity in the order of 10^{17} atm. Thus, it is possible to obtain in the void space high fugacities, while the pressure remains below that for cracking.

There is evidence that the phenomena reported depend upon the surface structure. Thus, the surface structure would determine the path and rate-determining step of deuterium evolution and this in turn is known to determine the fugacity developed in voids. Thus, the high fugacity in voids theory connects up the times of waiting for switch-on, the sporadicity of the results, and the fact that clean solutions do not give good results but dirty ones sometimes do.

5. References

1. K. Cedzynska and F.G. Will, Investigation of Cold Fusion Phenomena in Deuterated Metals, Final Report, Technical Information Series PB91175885, Vol I, p. I-80.
2. J.O'M. Bockris, D. Hodko and Z. Minevski, Proceedings of the II Annual Conference on Cold Fusion, p. 337, June 29 - July 4, 1991, Como, Italy.
3. G.H. Lin, R.C. Kainthla, N.J.C. Packham, O. Velev and J.O'M. Bockris, Int. J. Hydrogen Energy, 15 (1990) 537.
4. C.C. Chien, D. Hodko, Z. Minevski and J.O'M. Bockris, J. Electroanal. Chem., in press.
5. W. Beck, J.O'M. Bockris, J. McBreen and L. Nanis, Proc. Roy. Soc., A290 (1966) 220.
6. J. O'M. Bockris and P.K. Subramanyan, J. Electrochem. Soc., 118 (1971) 1114.
7. M.A. Fullenwider, Thesis, University of Pennsylvania, Philadelphia (1969).
8. J. O'M. Bockris, D. Hodko and Z. Minevski, presented at 180th Meeting of The Electrochemical Soc., Oct. 13-18, 1991.